Supporting Information

Pressure-dependent structure and electronic properties of energetic NTO crystal dominated by hydrogen-bonding interactions

Junyu Fan,[1,2] Pengju Wang[3,4] and Nan Gao[5,*]

[1]*Department of Physics, Taiyuan Normal University, Jinzhong, 030619, China*

[2]*Institute of Computational and Applied Physics, Taiyuan Normal University, Jinzhong, 030619, China*

[3]*Zhejiang Laboratory, Hangzhou 311100, China*

[4]*Key Laboratory of Materials Modification by Laser, Ion and Electron Beams (Dalian University of Technology), Ministry of Education, Dalian, 116024, China*

[5]*School of Materials Science and Engineering, Taizhou University, Taizhou 318000, China*

[*] Corresponding author. E-mail: gaonan@tzc.edu.cn

Table S1. The fractional atomic coordinates and lattice vectors of NTO at ambient condition.

lattice vectors	9.2413997650	0.0000000000	0.0000000000
	0.0000000000	5.5838999748	0.0000000000
	−1.5979251633	0.0000000000	8.8859687293
atomic coordinates	*x*	*y*	*z*
H_1	0.569580011	0.615239960	0.196170013
H_2	0.430420002	0.384760040	0.803830075
H_3	0.430419994	0.115239981	0.303830024
H_4	0.569580007	0.884760040	0.696169998
H_5	0.960030000	0.013049960	0.316989993
H_6	0.039969989	0.986950021	0.683010029
H_7	0.039969982	0.513049979	0.183010018
H_8	0.960029956	0.486950021	0.816990044
C_1	0.797939992	0.740069991	0.226899999
C_2	0.202059989	0.259930009	0.773100050
C_3	0.202059986	0.240069991	0.273100026
C_4	0.797939995	0.759930051	0.726900023
C_5	0.736450033	0.047369959	0.356929994
C_6	0.263549982	0.952630025	0.643070028
C_7	0.263549968	0.547369975	0.143070017
C_8	0.736450040	0.452630025	0.856930045
N_1	0.649829972	0.738939959	0.239230007
N_2	0.350170029	0.261059998	0.760770015
N_3	0.350170031	0.238940002	0.260770018
N_4	0.649829980	0.761059998	0.739230058
N_5	0.611710010	0.930219985	0.320190034
N_6	0.388289996	0.069779993	0.679810014
N_7	0.388289968	0.430220028	0.179809990
N_8	0.611710013	0.569779972	0.820190059

N_9	0.851850010	0.946269976	0.304790007
N_{10}	0.148150025	0.053730013	0.695209988
N_{11}	0.148150019	0.446269976	0.195210017
N_{12}	0.851850022	0.553730024	0.804790085
N_{13}	0.748460038	0.261870034	0.448280021
N_{14}	0.251540020	0.738129988	0.551720027
N_{15}	0.251540016	0.761870055	0.051719996
N_{16}	0.748460040	0.238129966	0.948280046
O_1	0.862450034	0.589519967	0.162850014
O_2	0.137550011	0.410480033	0.837150034
O_3	0.137549997	0.089519977	0.337149983
O_4	0.862449985	0.910479991	0.662850039
O_5	0.870559956	0.359689946	0.473120019
O_6	0.129440012	0.640310054	0.526880029
O_7	0.129440020	0.859689946	0.026879997
O_8	0.870560001	0.140310054	0.973119990
O_9	0.636480025	0.329949983	0.494569986
O_{10}	0.363520023	0.670050017	0.505430009
O_{11}	0.363520025	0.829949941	0.005430013
O_{12}	0.636479995	0.170050027	0.994570118

Table S2. Characteristics of vibrational modes in NTO crystal at ambient pressure. Abbreviation: asym: asymmetric, st: stretching, bend: bending, sci: scissoring, def: deformation, wag: wagging, tw: twisting, tor: torsion, rock: rocking.

Mode	Wavenumber/cm^{-1}					Assignment
	Expt.[S1]	A_g	B_g	A_u	B_u	
v_1		3140	3160	3139	3175	N-H st.
v_2		2841	2885	2844	2912	N-H st.
v_3		1649	1699	1663	1672	C=O st. + N-H bend.
v_4		1531	1535	1533	1532	N-H bend. + C-N st.
v_5		1462	1464	1453	1463	NO_2 asym. st + N-H bend. in plane
v_6	1395	1451	1452	1440	1442	N-H bend. in plane
v_7	1323	1399	1403	1396	1405	N-H bend. in plane
v_8	1271	1292	1303	1299	1298	N-H bend. in plane
v_9	1238	1265	1267	1265	1265	C-N st. + N-H bend.
v_{10}		1208	1217	1210	1212	C-N st. + N-H bend.
v_{11}	1090	1093	1089	1099	1091	C-N st. + N-H bend.
v_{12}	1000	984	1000	985	1000	C-N st. + N-H bend.
v_{13}		976	971	975	978	N-H bend. out of plane
v_{14}	881	894	914	875	887	N-H bend. out of plane
v_{15}	789	805	810	808	808	NO_2 sci. + Ring def.
v_{16}	754	741	759	739	754	N-H wag. out of plane + C-N st.
v_{17}	724	733	739	736	736	N-H wag. out of plane + C-N st.
v_{18}	710	723	733	724	733	N-H wag. out of plane
v_{19}	662	684	691	686	686	N-H wag. out of plane
v_{20}		602	593	606	589	Ring def. + N-H bend. in plane
v_{21}	571	574	574	574	575	Ring rock. + N-H bend. in plane
v_{22}	468	454	473	454	471	Ring def.
v_{23}	458	404	405	405	403	Ring def. + NO_2 sci.
v_{24}	339	335	341	343	335	Ring def. + C=O bend. out of plane
v_{25}	210	220	238	213	246	Ring def. + C=O bend. out of plane
v_{26}	186	186	161	176	184	Ring def. + C=O bend. out of plane
v_{27}	165	165	133	160	141	Ring def. +NO_2 tw.
v_{28}	137	151	116	144	125	Ring def. + NO_2 tw.
v_{29}		121	100	116	117	Ring def. + NO_2 tw.
v_{30}	77	96	82	96	88	Ring def. + NO_2 tor.
v_{31}		77	65	86	81	Ring def. + NO_2 tor.
v_{32}		29	48	31	38	Ring def. + NO_2 tor.
v_{33}		15	34	28	30	Ring def. + NO_2 tor.

Table S3. The frequencies of low-wavenumber vibrational modes (below 100 cm^{-1}) at ambient and pressure conditions.

Pressure/GPa	Wavenumber/cm^{-1}							
	Raman modes				IR modes			
	*v*30	*v*31	*v*32	*v*33	*v*30	*v*31	*v*32	*v*33
0	96	77	29	19	96	86	31	29
1	122	99	83	32	149	104	43	37
2	110	83	48	35	140	69	56	38
3	160	106	87	38	152	140	70	51
4	157	127	110	42	145	136	92	66
5	151	121	102	43	131	123	84	72
6	175	150	89	49	159	148	86	78
7	175	162	92	51	161	150	95	83
8	182	148	76	59	161	145	91	86
9	182	177	106	67	175	147	113	99
10	166	161	104	79	171	147	65	81
11	172	160	108	95	-	-	-	-
12	180	162	115	97	-	-	-	-
13	187	166	120	97	-	-	-	-
14	195	172	126	97	-	-	-	-
15	197	177	132	99	-	-	-	-

Table S4. The charge amount (*e*) on atoms at hydrostatic compression.

Pressure / GPa	C_1	C_2	N_1	N_2	N_3	N_4	O_1	O_2	O_3
0	0.67	0.81	4.55	6.25	6.69	8.13	6.45	6.46	8.00
2	0.66	0.81	4.56	6.24	6.69	8.12	6.46	6.47	7.99
4	0.65	0.82	4.57	6.23	6.70	8.09	6.47	6.47	7.98
6	0.63	0.83	4.59	6.21	6.71	8.07	6.50	6.50	7.96
8	0.63	0.84	4.59	6.20	6.72	8.06	6.51	6.50	7.95
10	0.61	0.84	4.60	6.19	6.72	8.05	6.53	6.51	7.95

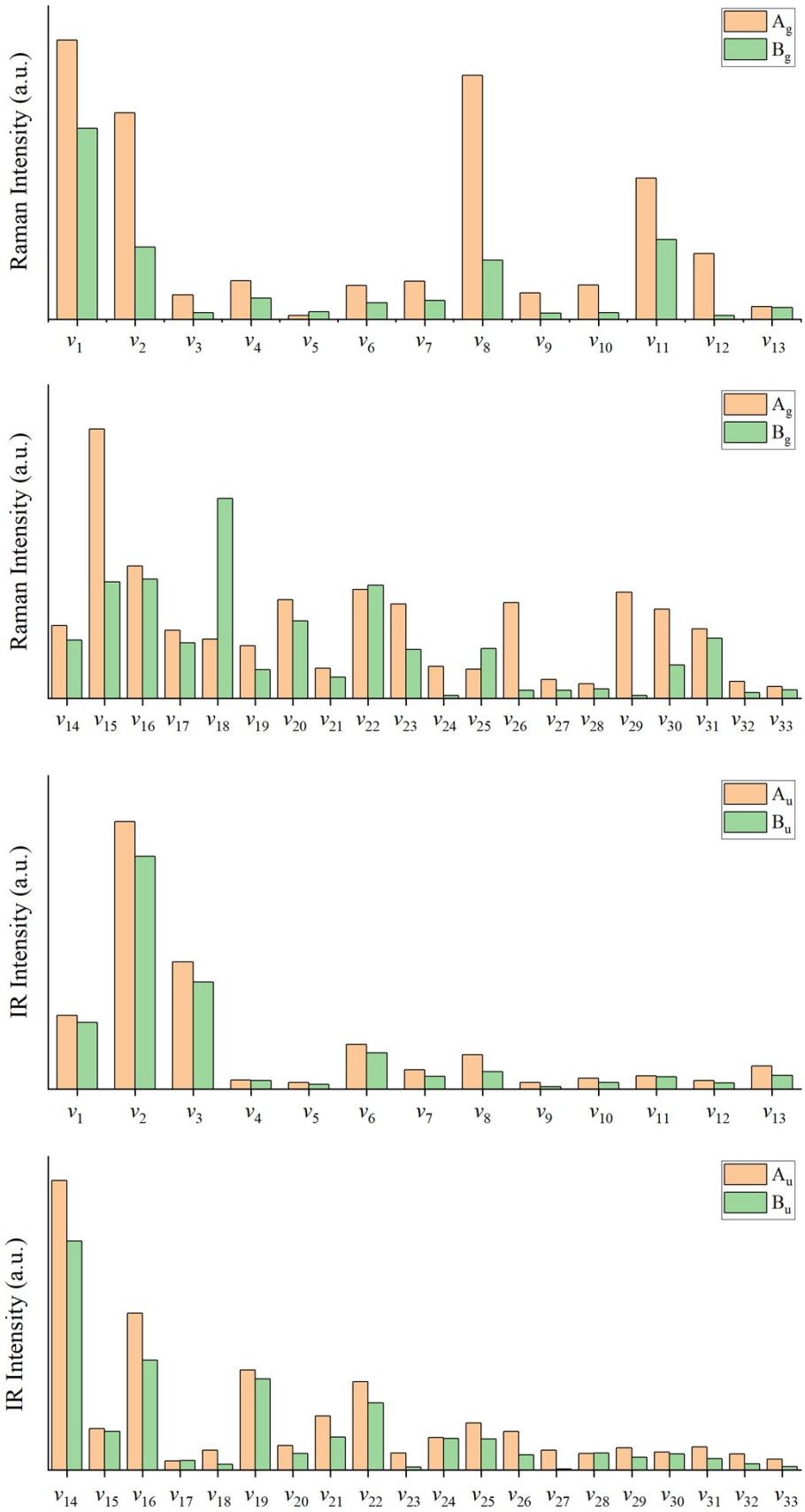

Fig. S1 The intensity of Raman and infrared modes with different symmetries (A_g, B_g, A_u, B_u).

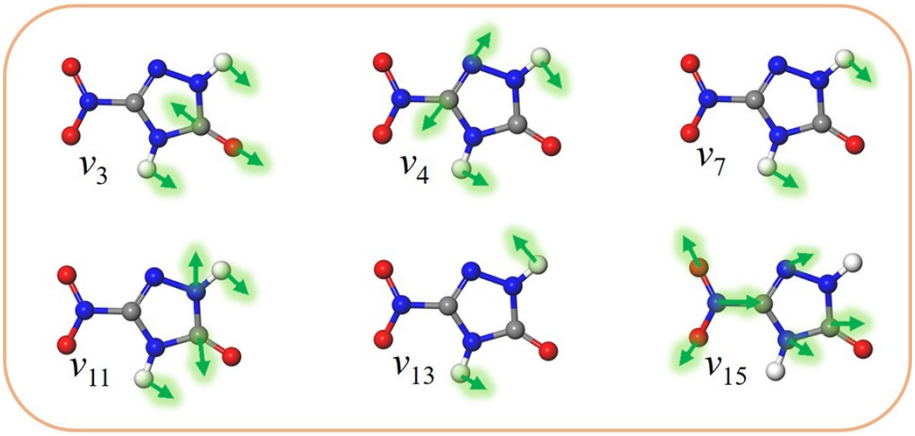

Fig. S2 The visualization of N−H bending modes $v_{7,13}$; and coupled with C=O stretching v_3, C−N stretching $v_{4,11}$ or O−N−O scissoring modes v_{15}.

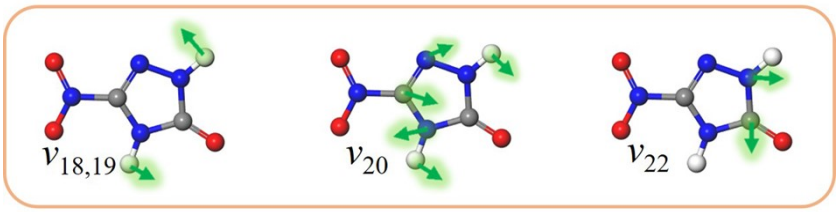

Fig. S3 The visualization of N−H wagging modes $\nu_{18,19}$; and coupled with ring deformation $\nu_{20,22}$.

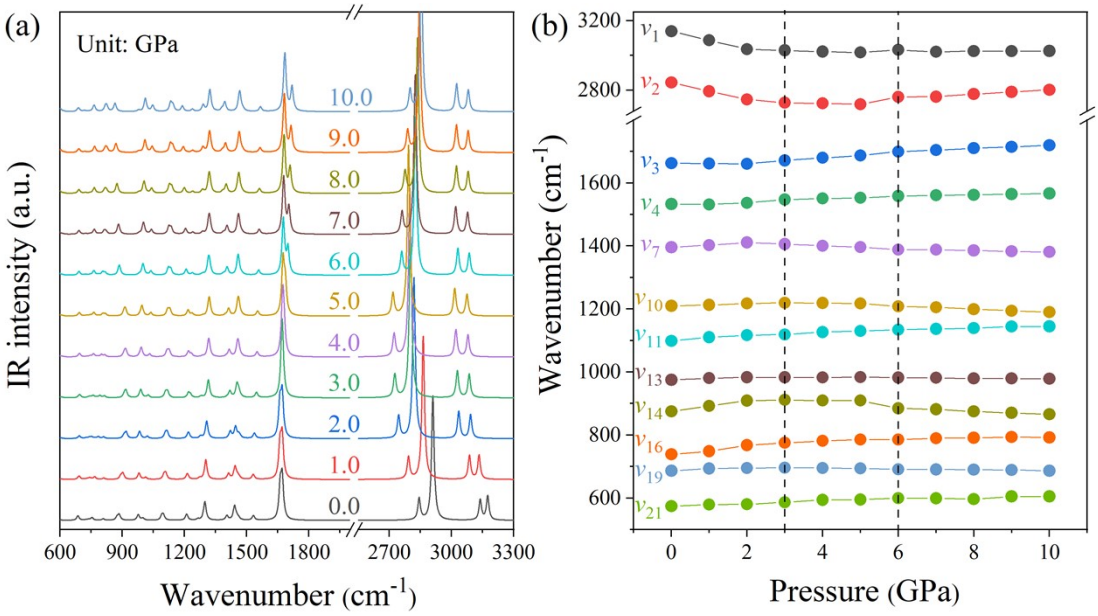

Fig. S4 (a) The variations of infrared spectra under hydrostatic pressure. (b) The wavenumber shifts of selected infrared vibrational modes under pressure.

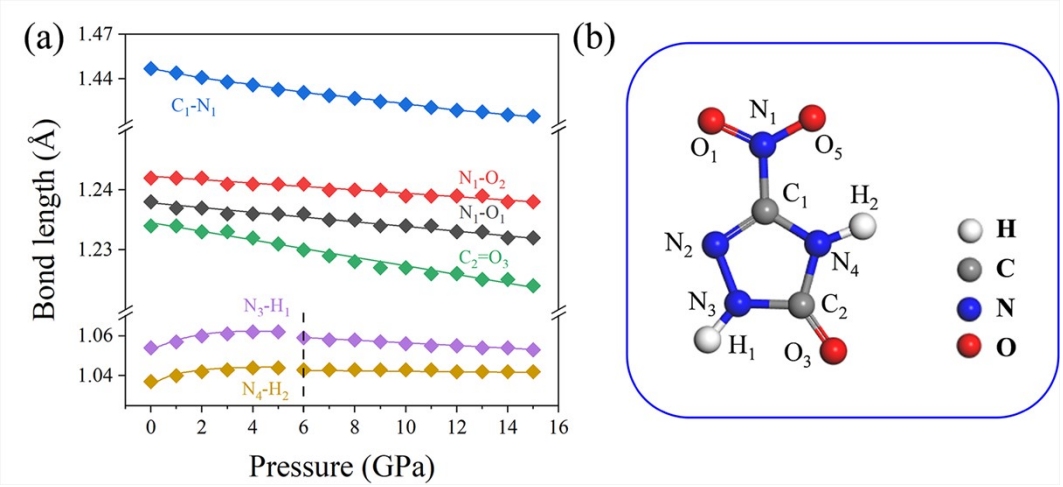

Fig. S5 (a) The evolution of molecular bond lengths under hydrostatic compression; (b) The atom serial numbers of NTO molecule are labeled.

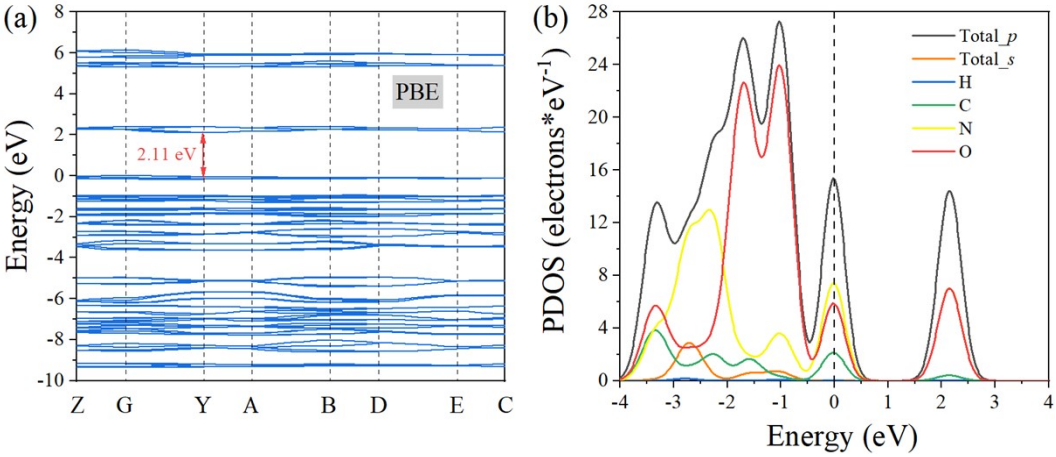

Fig. S6 The Energy band structure (a) and partial density of states (b) from PBE functional.

References

[S1] J. A. Ciezak and S. F. Trevino, *J. Mol. Struct.*, 2005, **732**, 211-218.